Article Post-Print

DOI: 10.1016/j.cep.2015.07.002 (2015)

Title: Design of dividing wall columns for butanol recovery in a thermochemical biomass to butanol process

Chinedu O. Okoli and Thomas A. Adams II*

Department of Chemical Engineering, McMaster University, 1280 Main Street West, Hamilton, Ontario

Abstract

In this work, ternary and quaternary dividing wall column (DWC) configurations for the separation of a multicomponent feed stream from a novel thermochemical lignocellulosic biomass to butanol process are designed, modeled and assessed. The goal is to separate the feed into four major products, with a key product being a biobutanol rich stream. Due to the complexity of DWC models, a shortcut modeling approach based on the minimum energy mountain method (also called the "V_{min} diagram method") is used to determine good initial values for the decision variables for the rigorous simulation of the DWC configurations. Furthermore, each DWC configuration is optimized to minimize the total annualized cost with the use of a derivative free algorithm coupled with a process simulator. The results show that the quaternary DWC configuration achieves up to 31 % energy savings, and 15 % capital savings in comparison to a conventional distillation sequence, and is thus a better option for implementation in the biofuel process.

* Corresponding author: Email: tadams@mcmaster.ca; Ph: (905) 525-9140 x24782

DWC, dividing wall columns; GA, genetic algorithm; HK, heavy key; LK, light key; MESH, material equilibrium summation and heat; MINLP, Mixed Integer Nonlinear Programming; NRTL, non-random two-liquid; PSO, particle swarm optimization; TAC, total annualized cost; VBA, Visual Basic for Applications; VLE, vapor liquid equilibrium; V_{min}, minimum energy mountain

Keywords: dividing wall column; biobutanol; V_{min} diagram; acyclic simulation structure; particle swarm optimization; total annualized cost

1. Introduction

As a result of global efforts to reduce emissions related to fossil fuel consumption, there has been a shift of focus to produce fuels from biomass. For example, the contribution of biofuels to total road-transport fuel demand was 3 % in 2013 and is estimated to grow to 8 % by 2035 [1]. However, to encourage further increase in the uptake of biofuels, production costs have to be reduced. One way to address this challenge is to reduce biofuel processing costs by employing cutting edge process intensification technologies such as dividing wall columns (DWC).

Since its first industrial application in 1985 by BASF, there have been more than one hundred DWCs implemented in industry, highlighting its increasing popularity [2], with past research showing that DWCs can reduce the investment and energy consumption of a multicomponent distillation process by up to 30 % in comparison to conventional distillation sequences [3–5].

Though DWC technology initially found wide application for distillation of zeotropic mixtures, its use has been further extended to other areas such as extractive distillation [6,7], azeotropic distillation [7,8] and reactive distillation [7]. Also critical to this uptake of DWCs is the fact that questions surrounding the controllability and operability of 3-product and 4-product DWCs have largely been addressed [4,9–12].

One important biofuel production process which may potentially benefit from the application of DWC technology is biobutanol production. This is because biobutanol, a gasoline substitute, is gathering increasing attention due to its advantages over bioethanol [13,14]. Recently, Okoli and Adams [15] showed that the fuel can be

produced at a cost of $0.83/L using a novel thermochemical process. That process used a train of conventional distillation columns in the separation section to separate an eleven component feed into four product blends (including a fuel-grade biobutanol product), and consumed 10% of the total energy and 8% of the total direct costs of the process. However, these energy and capital costs of the separation section can potentially be improved by utilizing DWCs for biobutanol recovery instead of conventional distillation columns, leading to a reduction in production costs of the process and thus have a significant impact in improving the competitiveness of biobutanol as a gasoline replacement. This application of DWC technology has not been previously investigated for biobutanol recovery from a thermochemical process, and is an interesting area of research as past research has demonstrated the benefits of DWC applications to bioethanol, bioDME and biodiesel production processes [16,17].

One major challenge in the research of DWC applications is their design. In commercial chemical process simulators the modeling of a DWC can be a difficult task as there are no custom DWC blocks. Methods identified from literature have made use of multiple columns in process simulators to represent different sections of the DWC [18,19]. Another challenge is the large number of internal column specifications needed for a DWC. This complexity means that computational difficulties should be avoided by using appropriate short-cut methods to determine initial estimates for the variables required for rigorous simulations. Once these variables have been estimated, rigorous simulations based on tray-by-tray MESH (material, equilibrium, summation and heat) equations can be implemented in the process simulation software. One such short-cut method is the minimum energy mountain method (also called the "V_{min} diagram method"). The V_{min} diagram method is a distillation column design tool that can be adapted and used to obtain good estimates for initializing rigorous DWC simulations. It

provides a graphical visualization of the minimum energy required for separation of a multicomponent zeotropic feed as a function of the feed properties [20]. The minimum energy is represented by the normalized vapor flow in the top section of the column, with the highest peak representing the minimum theoretical energy required for separation. The concept of the V_{min} diagram was introduced by Halvorsen and Skogestad of the Norwegian University of Science and Technology (NTNU) in a series of papers in 2003 [20–22]. The method was developed based on Underwood's equations, and requires only input feed details such as feed flowrate (F), composition (z) and feed quality (q) to estimate the minimum vapor flow in the top section of the column (V_T), and distillate (D) at infinite number of trays for desired product recoveries. The method can also be used to generate initial estimates for nonideal systems by using a process simulator and a large number of trays, typically around four times the minimum number of trays (N_{min}) [20].

Outside NTNU, this method has only been applied to the design of 4-product DWCs for multicomponent aromatics mixtures [19,23] and Sun and Bi [24] to the conceptual design of 3-product reactive DWCs. These papers demonstrated the efficacy of this method. However, as the number of applications of this method is limited, more independent validations are needed to demonstrate its potential.

In process design, the comparison of different design options is usually done based on identical criteria after an optimization has been carried out. Classical methods for optimizing DWCs are based on mathematical programming (which require derivative information) and fall into a class of problems known as Mixed Integer Nonlinear Programming (MINLP) problems. This is due to the presence of discrete variables such as feed location, and number of trays in different column sections, as well as the nonconvexity of the MESH equations. Javaloyes-Anton et al. [25], reviewed the

application of MINLP formulations for the solutions of complex distillation columns (including DWCs), and concluded that based on the high nonlinearities of these formulations, as well as sophisticated initialization techniques needed to obtain feasible solutions (only local optima are guaranteed as the solutions are highly dependent on the initialization points), these methods are complex and suited only for those skilled enough to adapt them for their own requirements.

An alternative, and easier to implement approach to these methods is to leverage the use of commercial process simulators and derivative-free or "black box" optimization algorithms. These derivative-free algorithms are typically population based, wherein the population contains individuals, with each individual representing a particular solution to the optimization problem. Once an algorithm termination criterion has been reached the optimization problem solution is chosen as that of the individual with the best objective function value. The advantage of these algorithms over derivative search methods is their ability to escape local optima and infeasibility regions, as well as provide multiple feasible solutions to account for real world considerations that are harder to quantify by the designer in an optimization setting. However, they are not able to guarantee that the solutions found are optimal. Though derivative-based search methods can theoretically offer local optimality guarantees, they are not easily amenable to highly complex real world problems and might be unable to find solutions which are as good as those obtained by derivative-free algorithms [25,26]. Examples of these derivative-free algorithms include genetic algorithms (GA), simulated annealing, particle swarm optimization (PSO) amongst others. In-depth discussions about these methods can be found in books, such as those written by Gendreau and Potvin [27], and Kaveh [28].

As a result of these advantages of derivative-free optimization algorithms over classical derivative search methods, the use of derivative-free optimization algorithms coupled with process simulators has found wide use in the literature for optimizing complicated process systems [25]. Amongst many examples in literature, Leboreiro and Acevedo [26] successfully demonstrated the use of a modified GA interconnected with the Aspen Plus process simulator to optimize complex distillation sequences including a Petlyuk column. Pascall and Adams II [29] made use of a PSO algorithm connected to Aspen Dynamics to optimize a novel semicontinuous system for the separation of DME from methanol and water. In that work PSO was used to optimize the controller tuning parameters of the system. The PSO algorithm coupled with Aspen Hysys was used by Javaloyes-Anton et al. [25] for the optimal design of conventional and complex distillation processes. In their work, the PSO algorithm implemented in MATLAB handles all the discrete variables such as the feed location and the number of trays in column sections, while continuous variables (reflux ratio, boilup ratio etc.) and product purity specifications are handled at the process simulator level. An interesting feature of their work was the use of a novel acyclic DWC simulation structure proposed by Navarro et al. [30] for representing a 3-product DWC in the process simulator. The use of an acyclic simulation structure over a traditional recycle structure reduces the simulation time in the process simulator, as the convergence of recycle tear streams is avoided. Despite the efficacy of their methodology, its application to DWCs was restricted to a relatively simple Benzene-Toluene-Xylene feed.

Based on this background, the objective of this paper is to investigate the benefits of applying 3-product and 4-product DWC technology to the recovery of fuel-grade biobutanol from a highly non-ideal multicomponent alcohol rich feed obtained from a thermochemical biobutanol process. The novelty of our work lies in the use of a

comprehensive methodology for designing the DWCs for this particular application. Firstly, we demonstrate how the V_{min} method can be used to estimate decision variables for acyclic 3-product and more complicated 4-product DWC simulation structures in Aspen Plus. Furthermore, the PSO algorithm coupled with Aspen Plus is then used to optimize the DWCs to minimize an economic objective function. In addition, a sensitivity analysis to investigate the importance of key parameters on the structure and economics of the best DWC configuration was also performed. To the best of our knowledge, this detailed approach for assessing and quantifying the potential for the application of DWC technology to biobutanol recovery is the first of its kind.

The rest of the paper is written as follows. Section 2 describes the system and design configurations under study, while in section 3 the design methodology is explained in detail. Subsequently, the results of the designed configurations are presented and analyzed in section 4. Finally, conclusions are drawn in section 5.

2. System Description

2.1 Feed and products

The multicomponent mixture to be separated is derived from a biobutanol synthesis process [15]. In this process, lignocellulosic biomass is converted to mainly biobutanol and other mixed alcohols through a number of processing steps consisting of biomass drying, gasification, syngas cleanup, and mixed alcohol synthesis. The resulting mixture undergoes a number of pre-distillation separation steps such as flashing to remove light gases, and water adsorption over a molecular sieve. Separation by distillation, which is the subject of this study, is then used to recover biobutanol and other mixed alcohols as products. Table 1 shows the components and feed conditions into the distillation system, as well as the product specifications.

Table 1: Feed, product and fixed column data for separation system

Feed conditions			**Fixed Distillation Column properties**	
Temperature (°C)	65.7		Condenser pressure	1.03 bar
Pressure (bar)	2.03		Tray pressure drop	0.01 bar/tray
Total Flow (kg/hr)	53,158		Tray efficiency	0.6
Total Flow (kmol/hr)	1,278			
q (feed quality, liquid fraction)	0.9			

Component	**Mole Fraction**	**Normal b.p. (℃)**	**Product cuts and specifications**		**Key components**
Carbon Dioxide	0.004	-109.2	A	> 99.3% mole recovery of Methanol	Methanol
Propane	0.036	-43.7			
Ammonia	0.001	-33.4			
n-Butane	0.057	31.1			
Methanol	0.683	64.7			
Ethanol	0.013	78.3	B	> 99% mole recovery of Ethanol	Ethanol, Propanol
Propanol	0.062	97.2			
Water	0.012	100.0			
Iso-Butanol	0.118	107.7	C	96% mole purity of Butanol [31]	Butanol
n-Pentanol	0.008	137.8	D	> 99% mole recovery of Pentanol	Pentanol
n-Hexanol	0.007	157.4			

2.2 **Design configurations**

In this study, several possible design configurations will be analyzed; a base case conventional configuration and three other DWC-based configurations. The distillation columns in all of the afore-mentioned configurations are simulated using the non-

random, two-liquid (NRTL) activity coefficient model with the Redlich-Kwong model for the gas phase and default binary interaction parameters provided in the simulator, Aspen Plus V8.0.

This model was chosen because it provided a good fit to experimental data for the most abundant alcohols (methanol to isobutanol) in the feed mixture (see Table 1). Specifically, the binary vapor liquid equilibrium (VLE) data of the methanol-isobutanol [32], ethanol-isobutanol [33], propanol-isobutanol [34], methanol-propanol [35], methanol-ethanol [36], ethanol-propanol [37] pairs were validated against experimental data. Furthermore, we note that the simulation did not detect two liquid phases using this model for any of the columns described in this study, and that there are no azeotropes present because of the very low water content in the feed.

2.2.1 **Base case**

There are five possible sequences of conventional binary distillation columns for the separation of a multicomponent feed into four products [38]. A quick way for identifying the most promising distillation sequence for further study is to apply the marginal vapor rate method [39] to determine the sequence with the least vapor flow rate. The vapor flow through the column provides a good indicator of both the column's capital and operating costs. This is because the reboiler and condenser duties increase with increased vapor flow, and larger vapor flows lead to larger diameter columns and thus higher capital costs. Therefore distillation sequences with lower vapor loads are preferred.

The results of the marginal vapor rate method as applied to the feed conditions and key component data provided in Table 1 are shown in Fig. 1. Each configuration is designed for 99.3 mol % recovery of key components, constant column pressure of 1 atm and a

reflux ratio of 1.2 times the minimum reflux ratio in each column. The vapor flow rates through each column shown in Fig. 1 are all normalized to the total feed flow rate. From Fig. 1 it can be seen that the direct sequence illustrated in Fig 1(a) has the least total vapor rate of 3.085. Thus this configuration is chosen as the base case for further detailed study.

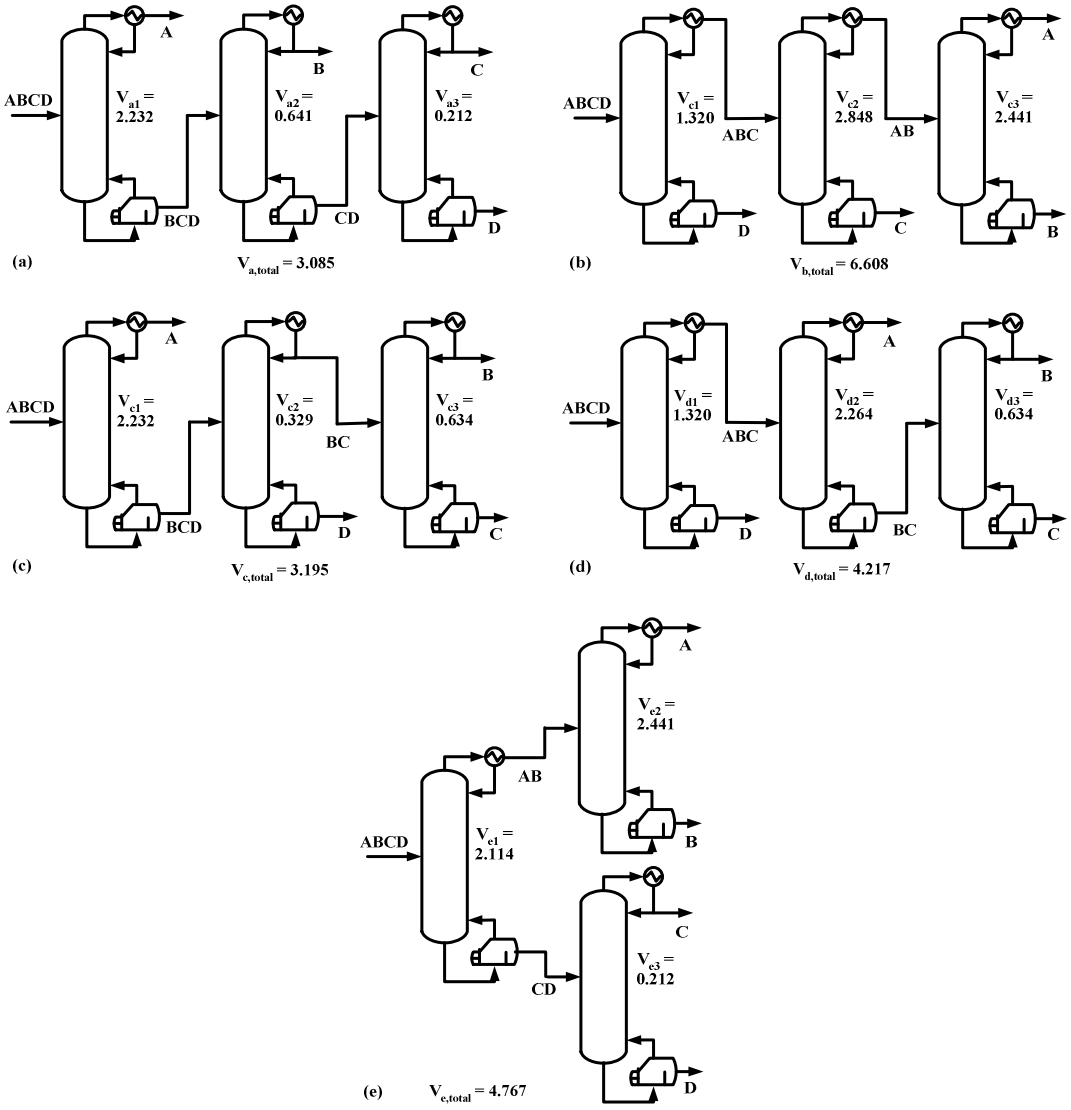

Figure 1: Conventional binary distillation column sequences for a 4-product recovery showing marginal vapor rate results (a) Direct sequence (b) indirect sequence (c) direct-indirect sequence (d) indirect-direct sequence (e) prefactionator arrangement.

2.2.2 **DWC configurations**

A DWC is a fully thermally coupled distillation sequence in which one condenser and one reboiler are used together with a single column containing one or more longitudinal partition walls, irrespective of the number of products required [19]. In the DWC, the internal re-mixing of streams which occurs in conventional columns is avoided, minimizing the entropy of mixing and thus energy required for separation of components [19]. The use of a single shell, reboiler and condenser to perform multicomponent (three or more components) separations in a DWC means that capital and energy costs of a distillation process can potentially be reduced.

Figs. 2 - 4 show three DWC configurations to be analyzed in this study. In Fig. 2 a DWC configuration with a conventional column for methanol recovery in direct sequence with a ternary product DWC is shown, while Fig. 3 shows a DWC configuration with a ternary product DWC in direct sequence with a butanol recovery column. Finally, Fig. 4 (a) shows a quaternary product DWC based on the Kaibel configuration i.e. using only a single partition wall [40]. The Kaibel configuration generally has a higher energy requirement than a 4- product Petlyuk configuration (Fig. 4 (b)) for the same quaternary product separation. However, the Kaibel column is preferred for practical implementation because it is easier to design, construct and operate, while the 4-product Petlyuk configuration has mechanical design, operational and control uncertainties that are yet to be overcome [19,41]. Therefore, the 4-product Petlyuk configuration is not chosen for this study.

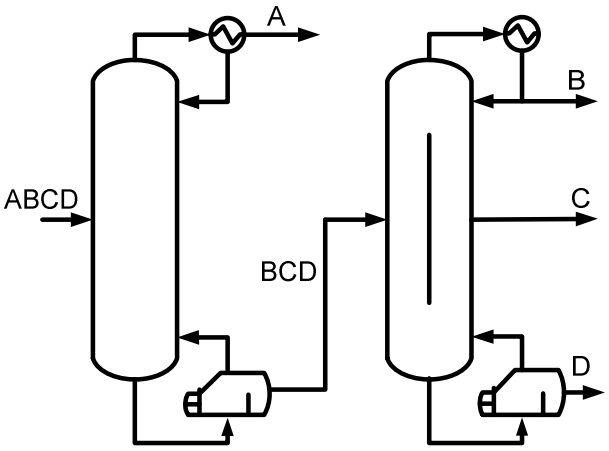

Figure 2: DWC configuration 1. Methanol recovery column and 3-product Petlyuk DWC

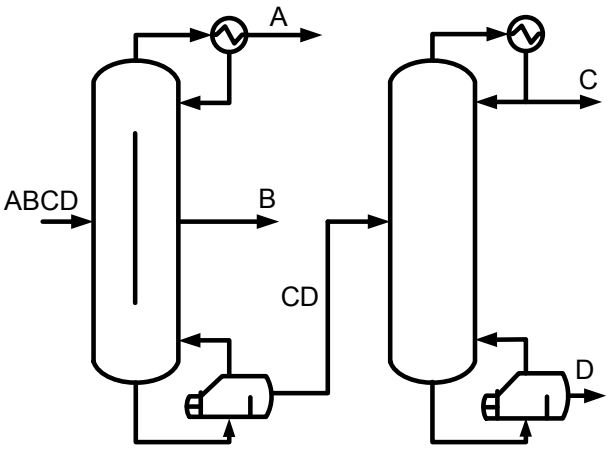

Figure 3: DWC configuration 2. 3-product Petlyuk DWC and butanol recovery column

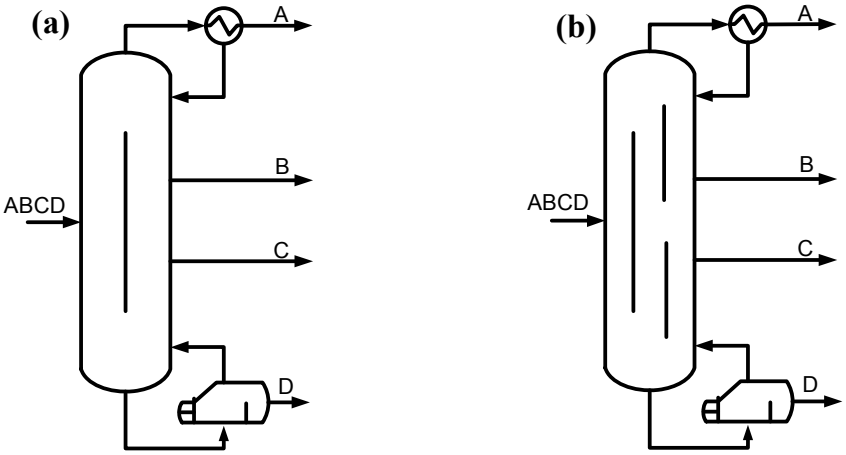

Figure 4: 4-product DWC using (a) the Kaibel configuration; (b) the 4-product Petlyuk configuration. The 4-product Petlyuk configuration is not used in this study except to help synthesize the Kaibel configuration.

3. Methodology

3.1 DWC simulation structure in process simulator

In process simulators, the traditional simulation strategy for DWCs is to represent the DWC structure as conventional columns in sequence connected by liquid-vapor recycle streams at the top and bottom of the column. This structure is also known as a recycle structure and is illustrated in Fig. 5 (a) for a ternary product DWC. In this structure, the first distillation column models the prefractionator section of the DWC, while the second column models the product sections of the DWC. In Aspen Plus, for example, each column in the model would be one RadFrac block. There are a number of disadvantages to this method; all related to the presence of recycle streams. The convergence of recycle streams when using the sequential modular mode of process simulators such as Aspen Plus is done through tear streams, thus at each iteration the columns and tear streams have to be converged leading to longer simulation times and a proneness to non-convergence. This is undesirable for scenarios where a flowsheet will undergo a large number of runs and robustness is a key criteria, such as when linked to an external optimization algorithm.

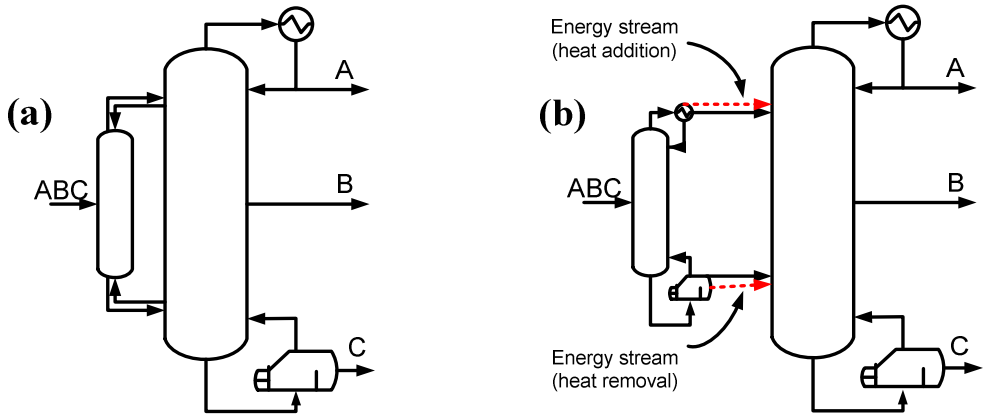

Figure 5: Two column structure options for the simulation of a ternary DWC: (a) recycle structure (b) acyclic structure

An alternative model structure for DWC simulation is the acyclic structure proposed by Navarro et al. [30], illustrated in Fig. 5 (b) for a ternary product DWC. In their work, the authors replace the material recycle streams present in the recycle DWC structure with material and energy streams. The top of the first column (prefractionator) is connected to the rectifying section of the second column (main column) with a vapor material stream at its dew point and an energy stream with the same energy that would have been removed if a partial condenser was used to provide reflux to the prefractionator. Furthermore, the bottom of the prefractionator is connected to the stripping section of the main column with a liquid material stream at its bubble point and an energy stream with the same energy that that would have been added if a reboiler was used to provide vapor to the first column. The acyclic structure avoids the problems associated with the presence of recycle streams in the recycle structure and thus simulates faster with easier convergence.

3.2 DWC initialization (minimum energy mountain (V_{min}) diagram method)

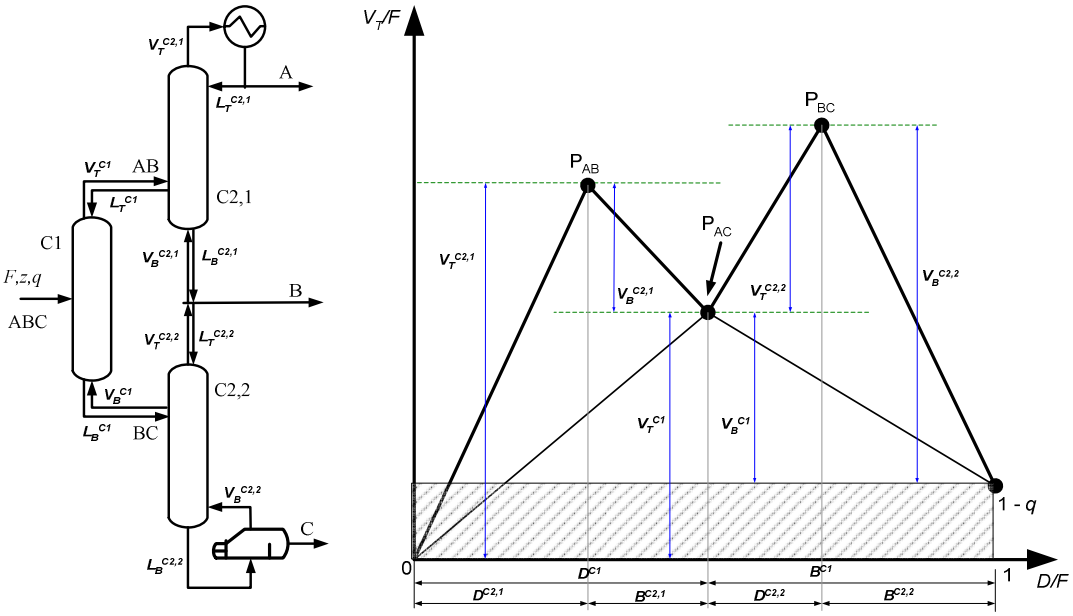

Figure 6: Example of column sections of a ternary DWC, and the V_{min} diagram

The V_{min} diagram method is used to generate good initial estimates of the design parameters for the DWCs discussed in this work using the following steps:

1. Select key components and their required recoveries (99.3 mol % is used in this study) for the given feed properties. For example from Table 1, for the separation between cut A and cut B, methanol is the light key (LK) component while ethanol is the heavy key (HK) component.

2. Calculate V_T/F and corresponding D/F values for all possible LK and HK splits between key components in a binary distillation column at constant pressure using at least $4N_{min}$ equilibrium stages at the specified recoveries. For example, to split a mixture of ABC in a single binary distillation column, there are three possible splits. (1) A/B, meaning that A is recovered in the distillate and B in the bottoms to the desired recoveries; (2) B/C, meaning B (and therefore A) in the distillate and C in the bottoms; and (3) A/C, meaning that A is in the distillate and C is in the bottoms to the desired

recoveries, with portions of B recovered in both. For each of these three cases, the distillate-to-feed ratio (D/F) and vapor-to-feed ratio (V_T/F) required to achieve the desired recoveries specified in step 1 (V_T is the vapor flow rate at the top of the column) are computed in a process simulator by assuming that the number of equilibrium stages is $4N_{min}$. For this study, a DSTWU model in Aspen Plus is used to compute N_{min} for each possible split, based on the classic Fenske equation. Then the DSTWU model is run a second time using $4N_{min}$ equilibrium stages to compute the feed location, D/F and reflux ratio. Next, this information is used as an initial guess for the more rigorous RadFrac model with $4N_{min} - 2$trays (tray efficiency is used) and the same feed location, but where the D/F and reflux ratio as predicted by DSTWU are used only as initial guesses for the design specification tool which varies D/F and the reflux ratio (RR) to achieve the desired product recoveries. The final values for D/F and V_T/F as computed by RadFrac are plotted on the V_{min} diagram as shown in Figure 6, where points P_{AB}, P_{BC} and P_{AC} correspond to the solutions for the A/B, B/C, and A/C splits, respectively. Note, for quaternary systems, there would be six points instead of three, corresponding to splits of A/B, A/C, A/D, B/C, B/D, and C/D.

3. Using V_T and D computed from step 2 for each split in a binary distillation column, the corresponding liquid flow at the top of the column (L_T), the liquid flow at the bottom (L_B), the vapor flow at the bottom (V_B), and the bottoms flow rate (B) can be computed using the material balance equations (1) – (4):

$$L_T = V_T - D \tag{1}$$

$$L_B = L_T + qF \tag{2}$$

$$V_B = V_T - (1-q)F \tag{3}$$

$$B = F - D \quad (4)$$

These flows are depicted graphically in Fig. 6 for the column sections of a ternary DWC.

4. The corresponding operating variables such as *RR* and boilup ratios (*BR*) which are useful for initializing the DWC simulation structure can then be computed using equations (5) – (6), while the side flowrate(s) can be calculated via an appropriate material balance.

$$RR = L_T / D \quad (5)$$

$$BR = V_B / B \quad (6)$$

3.3 **Derivative-free Optimization algorithm**

The PSO algorithm is a derivative-free optimization technique inspired by nature. The algorithm mimics the way a swarm of birds (particles) locate a best landing place. In the algorithm, the velocity and position of each particle in a swarm is updated iteratively based on its (i) past velocity and position (ii) personal best position at each iteration (iii) global best position (swarm's best) at each iteration. The algorithm is terminated once a stopping criterion is satisfied, and the global best position is subsequently outputted as the optimum. Adams II and Seider [42] demonstrated the effectiveness of the PSO algorithm for the practical optimization of complex chemical distillation processes. Apart from its effectiveness, it is also chosen for this work because it is easy to implement and use with commercial simulation software, and has few tuning parameters.

For this work a discrete version of the PSO algorithm in which discrete decision variables are treated as continuous variables for use in the PSO algorithm, but rounded

to the nearest integer (or discrete value) when used to evaluate the objective function (that is, to run the simulation) [43]. Furthermore, the positions of the particles are initialized using a Latin hypercube sampling method to enable adequate sampling of the search space.

3.4 **Objective function**

Table 2: Additional data for capital and utility costs calculations

Distillation columns (default values from Aspen Plus V8.0**)**	
Tray type: sieve tray	
Tray spacing, *s*: 0.609 m	
Column height, *H* (m) = 3 + (*NT* × *s*); where *NT* = number of trays	
Flooding approach: 80 % [44]	
Utility costs	
Natural gas [45]	\$2.38/GJ
Electricity [46]	\$0.0491/kWh
Water makeup and treatment [47]	0.0005 cents /L
Steam, computed cost (10 bar medium pressure steam, 185 °C)	\$2.14 /GJ
Cooling water, computed cost (30 – 45 °C)	\$0.278 /GJ

The basis of comparison of the design configurations is the total annualized cost (TAC) of each design, which is minimized as the objective function of the PSO algorithm. The TAC for each column is a sum of the operating cost per year and annualized capital cost of the column, assuming an annualization period in years. The operating cost is the cost of the utilities (steam and cooling water) needed to provide the required heating and cooling duties to the column reboiler and condenser. These costs are estimated using the method described by Towler and Sinnott [47] in which the prices of steam (medium pressure) and cooling water are directly related to the prices of natural gas, electricity

and water (see Table 2 for references).The capital cost is dependent on the column diameter, number of trays, and heat exchanger areas. Correlations for computing the costs of the reboiler, condenser, and sieve trays are obtained from Seider et al. [38], while cost correlations for the column are obtained from Rangaiah et al. [48]. Dejanovic et al. [9] recommends that the sieve trays in the dividing wall section of the DWCs should be about 1.2 times the cost of conventional sieve trays. Instead, it was assumed that the cost is 1.5 times the cost of conventional sieve trays as a conservative estimate. These sieve trays are specially constructed with partition walls for use in DWCs with non-welded walls. Dejanovic et al. [9] notes that they are becoming more popular in DWCs as they allow much more design and implementation flexibility. The material of construction is assumed to be carbon steel for all capital cost computations. The computed capital cost is subsequently annualized by multiplying with an annualization factor (*f*) using equation (7), where *i* is the fractional interest rate per year, and *n* is the annualization period in years. The values of *i* and *n* are set at 0.1 (or 10 %) and 5 years respectively as recommended by Smith [49].

$$f = \frac{i(1+i)^n}{(1+i)^n - 1} \tag{7}$$

In order to consistently compare the predicted costs of the DWC systems in this work to the costs of the conventional continuous distillation sequences, the cost year for the analysis is December 2012 with an operating time of 8,000 h/yr for all cases. Other data for the computation of the capital and utility costs are shown in Table 2.

3.5 Two tier simulation - optimization implementation algorithm

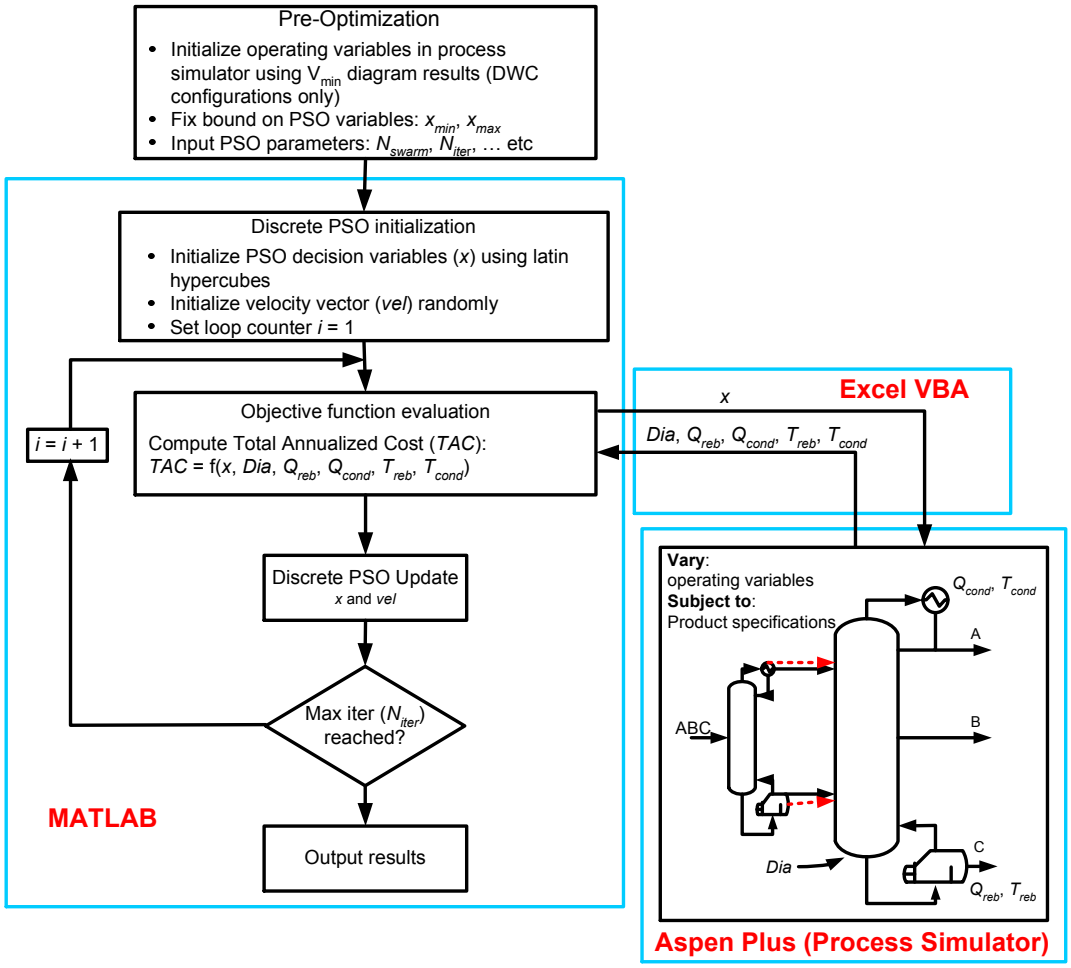

Figure 7: Illustration of the implemented algorithm

The proposed design methodology is implemented as illustrated in Fig. 7. The objective is to determine the optimal structure (feed location, total number of trays) and operating conditions (*RR*, *BR*) of the distillation columns that minimize the TAC while achieving product specifications. The implementation starts at the pre-optimization stage. For the DWC configurations, the V_{min} method is used to determine the initial values for the operating variables of the acyclic DWC simulation structure (equilibrium-based RadFrac models in Aspen Plus are used to represent the columns). Subsequently, input parameters and bounds on the decision variables of the PSO algorithm are fixed. Each decision variable, N_j, represents the number of trays in the jth section of the product

column. Where j is a subset of J (the total number of sections in the product column). An additional decision variable for the DWCs only is N_{J+1}, which represents the tray number of the feed location into the prefractionator. These values are then inputted into MATLAB.

For the DWC configurations, the number of trays from the V_{min} computations are used to determine the upper bounds of the number of trays in each column section for the PSO algorithm using a heuristics approach. First, the upper bounds are fixed from the V_{min} results. For example, for DWC configuration 1, the upper bound of the number of trays in N_I is fixed at from column section C2,1 from the V_{min} results (see Fig 13 for decision variable, and Table 4 for V_{min} results). The upper bound on N_{II} is fixed at $NT - N_{feed}$ from column section C2,1 i.e. the bottom half of the column. In addition the upper bound on N_{III} is fixed at N_{feed} from column section C2,2, while the upper bound on N_{IV} is fixed at $NT - N_{feed}$ from column section C2,2. Finally, in runs where the particles get stuck at the upper bound, these bounds are increased. The bounds can also be tightened to reduce the search space.

The PSO algorithm implementation in MATLAB then proceeds as follows; first, the decision variables of the PSO algorithm are initialized using a Latin hypercube sampling technique applied to the search space created by the bounds on the decision variables. Once the initialization of the decision variables is complete, their values are then passed to the Aspen Plus based process simulator via an Excel Visual Basic for Applications (VBA) interface. The information received from Excel VBA is used to specify the structure and feed location of the distillation columns in the process simulator. Note again that the decision variables of the PSO algorithm are discrete, and so although the variables are treated as continuous in the PSO algorithm, they are rounded to the nearest integer before passing them to Aspen Plus. Furthermore, the

distillation columns in Aspen Plus are set up to meet recovery or purity specifications of key components in product streams (distillate, bottom, and side streams as shown in Table 1) by varying operating variables such as reflux ratios, boilup ratios and flowrates of side streams. Thus, Aspen Plus handles all the operational constraints. Furthermore, the tray efficiencies (shown in Table 1) are also accounted for in the distillation column structure set up in Aspen Plus. The simulation is then run in Aspen Plus which returns information to MATLAB (via the Excel VBA interface) such as column diameter (*Dia*), reboiler and condenser duties (Q_{reb} and Q_{cond}), and reboiler and condenser temperatures (T_{reb} and T_{cond}) needed to compute the TAC. The TAC is then evaluated using the column structure information from the PSO algorithm and information from the process simulator. Based on the results of the TAC computation, the PSO decision variables are updated and passed to the process simulator via the Excel VBA interface. This process between MATLAB, which houses the PSO algorithm and TAC objective function, and Aspen Plus process simulator continues iteratively until an algorithm termination criteria is met i.e. a certain number of iterations has been completed by the PSO algorithm. In addition, a large penalty coefficient is used to penalize the objective function in cases of infeasible or failed runs of the process simulator (runs ending with errors). For all the cases studied in this work ten particles are chosen for the PSO algorithm, with the number of iterations (per particle) set to be one hundred.

4. Results and discussion

4.1 V_{min} diagram results

4.1.1 V_{min} diagram results for DWC in configuration 1

Table 3: Properties of the feed into the DWC of configuration 1

Feed conditions			
Temperature (°C)	120.3		
Pressure (bar)	2.06		
Total Flow (kg/hr)	18,776		
Total Flow (kmol/hr)	284		
q (feed quality, liquid fraction)	0.86		
Mole Fraction, *z* (-)		**Product cuts**	**Key components**
Methanol	0.021	B	Propanol
Ethanol	0.056		
Water	0.055		
Propanol	0.276		
Butanol	0.527	C	Butanol
Pentanol	0.036	D	Pentanol
Hexanol	0.029		

In configuration 1, methanol and lighter gases (cut A) have been removed at the top of the conventional column, and the resulting bottoms are sent to the DWC. The properties of the resulting feed into the DWC are shown in Table 3.

Fig. 8 shows the column sections and the resulting V_{min} diagram for the DWC in configuration 1. The highest peak occurs at P_{BC}, meaning that the separation between cuts B and C is the most difficult and thus requires the most energy. This is expected, as

amongst the key components shown in Table 3 the boiling points of propanol and butanol are the closest and will thus be the most difficult separation in comparison to the others.

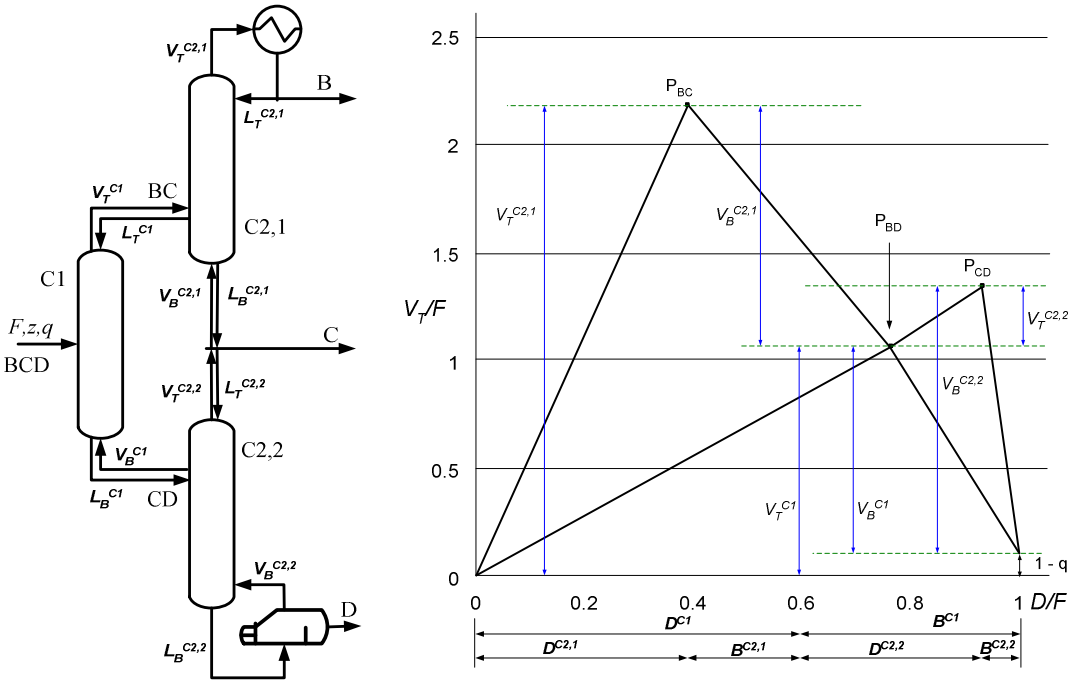

Figure 8: column sections and V_{min} diagram results (not drawn to scale) for DWC configuration 1

The V_{min} diagram results are then used with equations 1 – 6 to calculate all the flows in the column sections illustrated in Fig. 8, and to subsequently compute the reflux ratios, boilup ratios, and side flowrate required for initializing the acyclic DWC structure. Table 4 shows the results of these calculations for normalized flows (based on the feed flowrate).

For initializing the operating variables in the acyclic DWC structure the required values for the product column are $RR^{C2,1}$, $BR^{C2,2}$ and side stream flowrate (sum of $D^{C2,2}$ and $B^{C2,1}$). While for the prefractionator, RR^{C1} and BR^{C1} are used.

Table 4: Calculated material balance results for the V_{min} diagram in Fig. 8 (all flows are normalized by dividing with *F*)

Sections	**C2,1**	**C2,2**	**C1**
NT	100	40	28
N_{feed}	50	20	14
Specified from V_{min} diagram			
V_T	2.2266	0.1945	1.1333
V_B	1.0933	1.1895	0.9950
D	0.4107	0.1406	0.7909
B	0.3802	0.0684	0.2091
Calculated			
L_T	1.8158	0.0539	0.3424
L_B	1.4734	1.2579	1.2041
RR	4.4207	0.3831	0.4329
BR	2.8757	17.3826	4.7588

4.1.2 V_{min} diagram results for DWC in configuration 2

The properties of the feed into the DWC in configuration 2 are shown in Table 1. However, cut C now comprises of pentanol and hexanol, as butanol and all components heavier than it are recovered in the bottom of the column. The column sections and resulting V_{min} diagram results are illustrated in Fig. 9. The highest peak is P_{AB}, which represents the energy required for the separation of cuts A and B, for which methanol is the light key from cut A and ethanol is the heavy key from cut B.

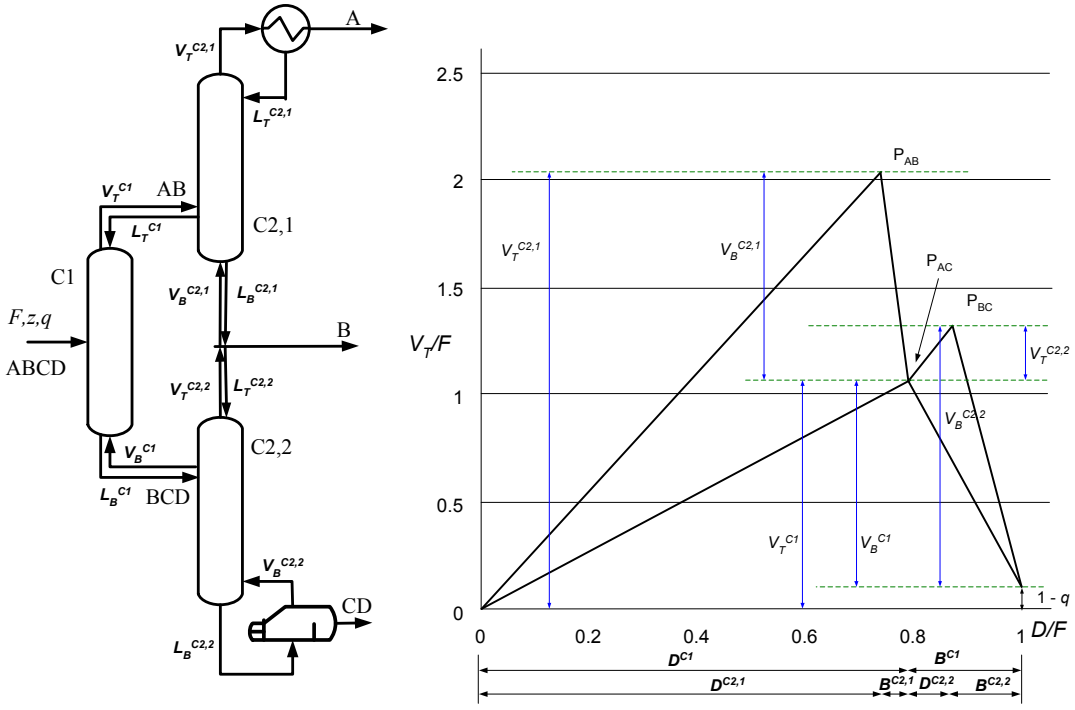

Figure 9: column sections and V_{min} diagram results (not drawn to scale) for DWC configuration 2

Table 5 shows the results of the calculations based on equations 1 – 6. The selection of *RR* and *BR* values for initializing the acyclic DWC structure, as well as the calculation of the side stream flowrate is the same as that described in section 4.1.1.

Table 5: Calculated material balance results for the V_{min} diagram in Fig. 9 (all flows are normalized by dividing with *F*)

Sections	**C2,1**	**C2,2**	**C1**
NT	108	99	40
N_{feed}	47	45	18
Specified from V_{min} diagram			
V_T	2.0192	0.2255	1.0256
V_B	0.9936	1.1531	0.9276
D	0.7753	0.0772	0.7902
B	0.0149	0.1326	0.2098
Calculated			
L_T	1.2439	0.1484	0.2354
L_B	1.0085	1.2857	1.1374
RR	1.6044	1.9220	0.2979
BR	66.7094	8.6957	4.4215

4.1.3 V_{min} diagram results for DWC in configuration 3

The properties of the feed into the DWC in configuration 3 are shown in Table 1. The methodology described in section 3.2 for generating the V_{min} diagram is sufficient for Petlyuk configurations, as is the case in configurations 1 and 2. However, for the Kaibel configuration used in configuration 3, an additional step is taken to generate the V_{min} diagram from its corresponding 4-product Petlyuk configuration (see Figure 4). This is because unlike the Petlyuk configuration, the prefractionator of the Kaibel configuration does not perform the easy split between products A and D, but performs the more difficult split between products B and C [50].

The procedure for generating the V_{min} diagram of the Kaibel configuration from its corresponding Petlyuk configuration is illustrated in Fig. 10, and is done using the

graphical method described by Halvorsen and Skogestad [50], which is again based on the Underwood equations.

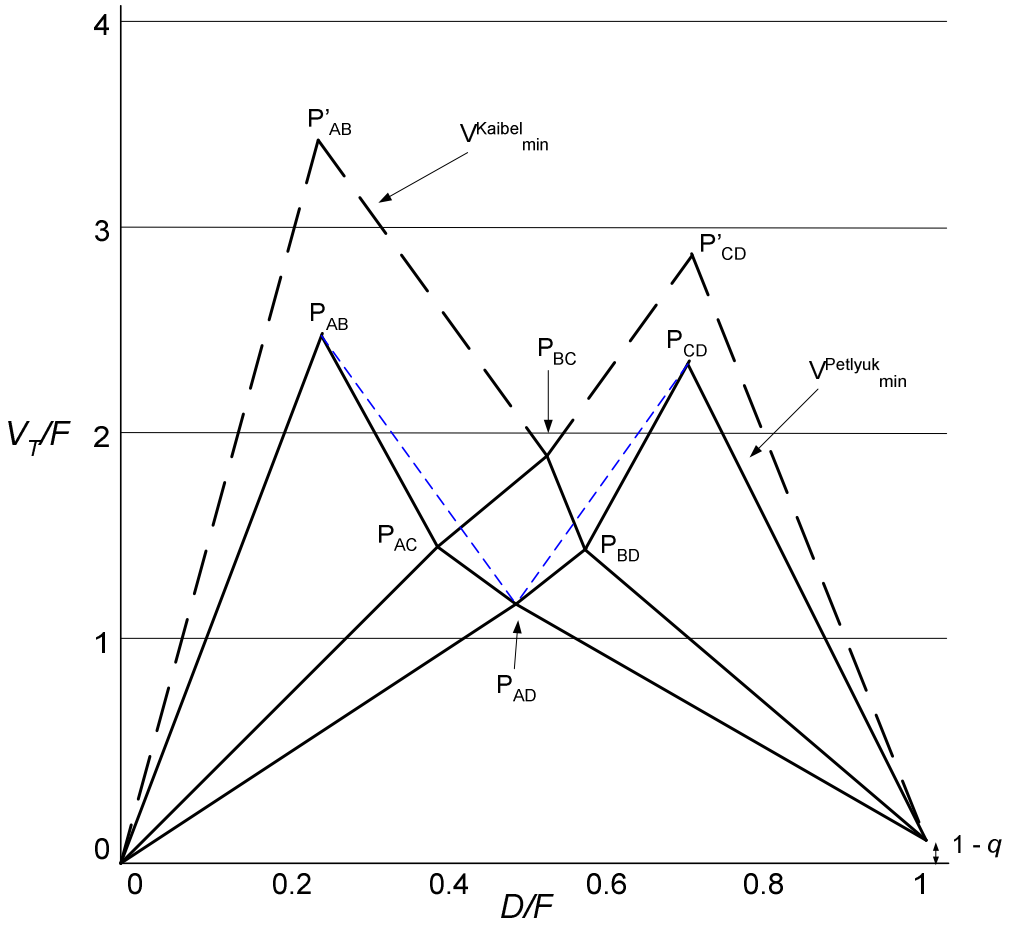

Figure 10: Illustration of V_{min} diagrams (Kaibel and Petlyuk) for a 4-product DWC

First the V_{min} diagram for the 4-product Petlyuk configuration is generated using the methodology described in section 3.2. The resulting V_{min} diagram is shown with the solid lines in Fig. 10, with peaks at P_{AB}, P_{BC}, and P_{CD}. The point P_{BC} is shared by both the 4-product Petlyuk and Kaibel configurations, as the prefractionator in the Kaibel column performs the split between B and C. To obtain approximate locations for peaks P'_{AB} and P'_{CD}, draw lines parallel to $P_{AD}P_{AB}$ and $P_{AD}P_{CD}$ (shown in Fig. 10 as dashes) from P_{BC} to intersect at the vertical lines through P_{AB} and P_{CD}. The intersection of these

parallel lines from P_{BC} with the vertical lines through P_{AB} and P_{CD} give the peaks P'_{AB} and P'_{CD} respectively for the Kaibel configuration.

By applying the procedure discussed above, the V_{min} diagram result for configuration 3 can be obtained, and is shown in Fig. 11. The broken lines outline the V_{min} diagram of the Kaibel configuration, while the solid lines show the V_{min} diagram of the corresponding 4-product Petlyuk configuration. The highest peak occurs at P'_{AB} which as mentioned before is the separation between methanol in cut A, and ethanol in cut B.

The middle section (C2x) of the product column in the Kaibel column performs the sharp B/C split [51]. However, as this has already been performed in the prefractionator, the number of trays in this section is computed as the minimum number of trays using the Fenske equation.

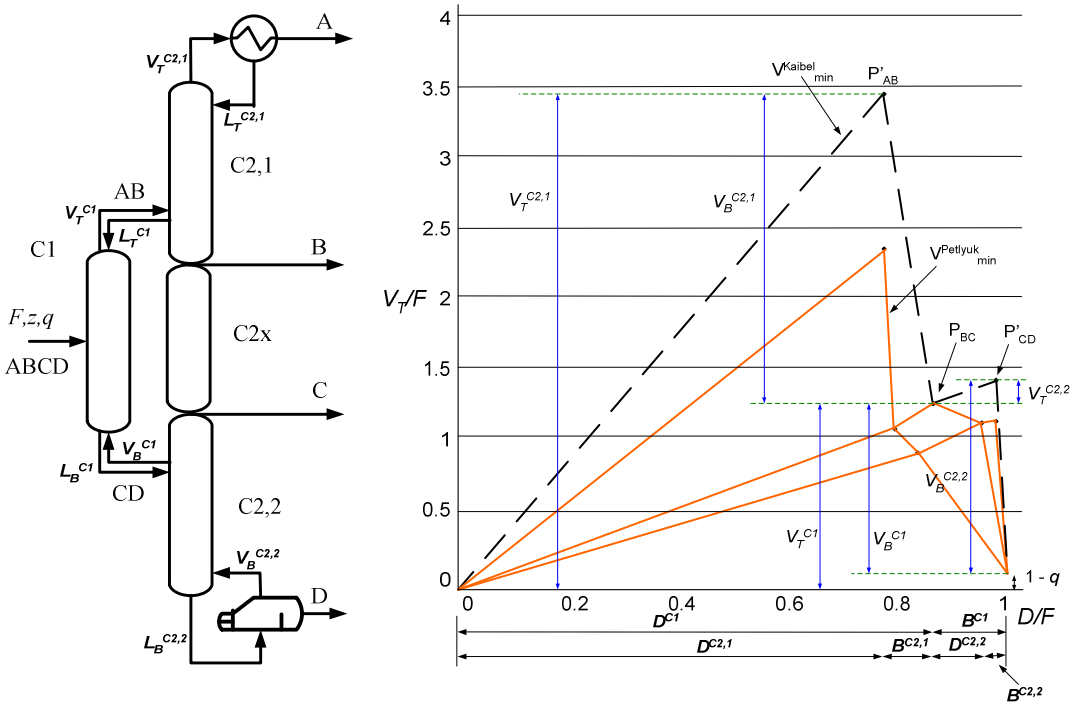

Figure 11: column sections and V_{min} diagram results (not drawn to scale) for DWC configuration 3. Kaibel column (broken lines) and Petlyuk column (solid lines) are shown.

The material balance calculations for the V_{min} diagram are shown in Table 6.

Table 6: Calculated material balance results for the V_{min} diagram in Fig. 11 (all flows are normalized by dividing with *F*)

Sections	**C2,1**	**C2,2**	**C1**
NT	108	99	40
N_{feed}	47	45	18
Specified from V_{min} diagram			
V_T	3.4375	0.1864	1.2511
V_B	2.1864	1.3404	1.1540
D	0.7753	0.1168	0.8674
B	0.0921	0.0158	0.1326
Calculated			
L_T	2.6622	0.0695	0.3837
L_B	2.2784	1.3561	1.2866
RR	3.4337	0.5950	0.4424
BR	23.7443	84.9916	8.7021

For initializing the operating variables in the acyclic DWC structure the required values for the product column are $RR^{C2,1}$, $BR^{C2,2}$ and side stream flowrates ($D^{C2,2}$ and $B^{C2,1}$). While for the prefractionator, RR^{C1} and BR^{C1} are used. Note that unlike in the other DWC configurations, there are two side stream flowrates in configuration 3.

4.2 **Optimization results (optimal structures)**

4.2.1 **Base case**

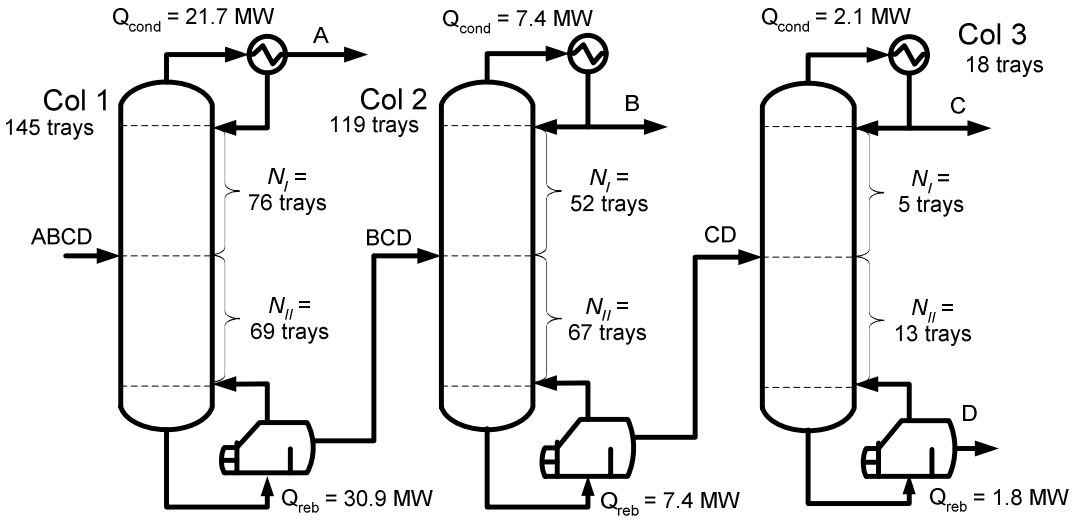

Figure 12: Base case showing the optimal structure of the columns, and condenser and reboiler duties

The base case is set up using the data shown in Table 1 with the results of its optimal structure shown in Fig. 12. For the base case each column is optimized individually. Each column is divided into 2 column sections with the number of trays in each column section as decision variables (N_I and N_{II}). Furthermore, the bounds of each decision variable were kept between 4 and 80 for the optimization. In addition, it should be noted that the PSO was re-run using a variety of different sets of initial conditions for the swarm, but the algorithm always converged on the same optimum result. The results show that the first column which recovers methanol and lighter components (cut A) in the distillate is the largest, both in terms of number of trays, and condenser and reboiler duties. The higher energy requirement in this column can be explained by the larger flowrate into the first column, the large amount of methanol in the feed (68.3 mol %), and the close boiling point between methanol and ethanol (HK component in cut B). All these make recovering > 99.3 % mole recovery of methanol in the distillate difficult and

more energy intensive in comparison to the other columns. Note also that though this column is tall, at approximately 91.3 m, it is below 110 m (about 175 trays) which is the maximum height recommended for distillation columns [41].

4.2.2 **DWC configurations 1 and 2**

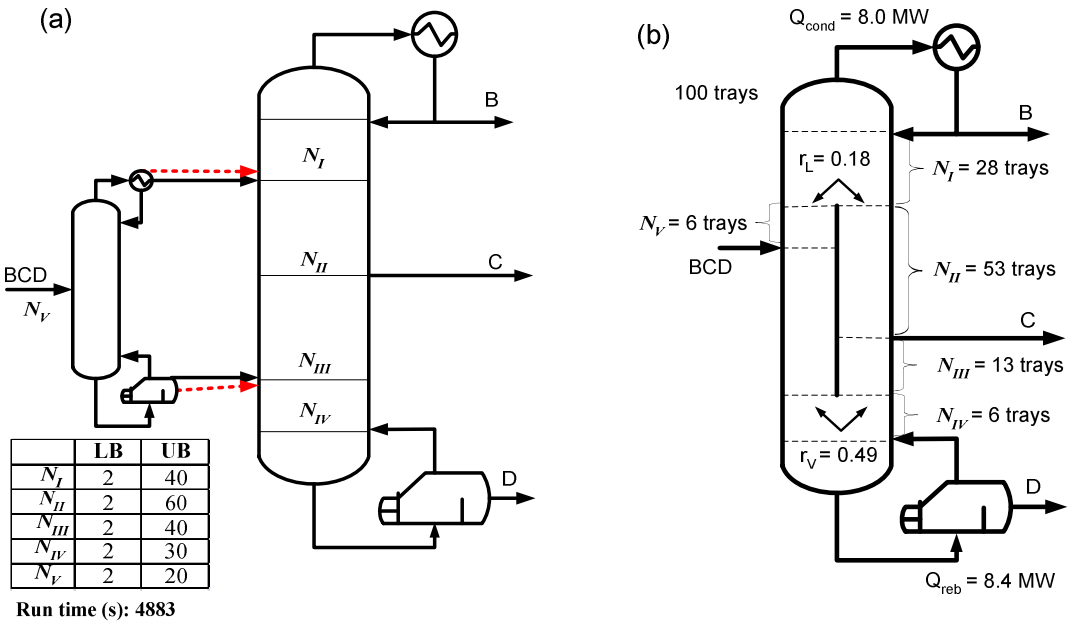

Figure 13: Model for DWC configuration 1 showing (a) simulation structure, with PSO variables and bounds (b) optimal structure of the equivalent DWC design with the condenser and reboiler duties, liquid split ratio (r_L) and vapor split ratio (r_V)

In DWC configuration 1, the first column is a conventional methanol recovery column with specification and results as discussed for column 1 of the base case in section 4.2.1. The output of that column, with feed properties as shown in Table 3, is subsequently fed into the 3-product DWC. In comparison to a conventional column, there are additional operating and structural variables for minimizing the TAC of the DWC. This is because of the presence of a side stream in the DWC, as well as the interconnection between the prefractionator and product columns of the DWC. In the process simulator, five operating variables need to be specified for simulating the acyclic DWC structure.

These are the *RR*, *BR* and side stream flowrate of the product column, as well as the *RR* and *BR* of the prefractionator. The initialization of these variables is done using the results of the V_{min} method shown in section 4.1.1. In the process simulator setup the operating variables of the product column are varied to meet the specifications of the product streams (*RR* for B, side stream flowrate for C, and *BR* for D). This leaves the two operating variables of the prefractionator as degrees of freedom which can be varied to minimize the reboiler duty. However, in this study we simplify the process simulator setup and leave the values of *RR* and *BR* of the prefractionator at their V_{min} result values. To optimize the 3-product DWC structure, five independent discrete variables are used as shown in Fig. 13 (a) with their respective bounds. Variables N_I - N_{IV} relate to the number of trays in the sections of the product column, while variable N_V relates to the feed location at the prefractionator. In reality the prefractionator of the DWC is in fact located in the product column; thus a simplifying assumption is that the number of trays in the prefractionator is equivalent to the number of trays in the corresponding part of the product column i.e. the summation of variables N_{II} and N_{III}. This assumption means that an over-separation will be performed on one side of the dividing wall. However, the approach is still very reasonable as the most difficult separations determine the height of the DWC. The resulting optimal structure after optimization is shown in Fig. 13 (b).

In DWC configuration 2, the DWC column is placed before a conventional column for butanol recovery. Apart from the difference in feed properties into the DWC column, its process simulation setup and optimization is similar to that of the DWC column in configuration 1. The structure setup and optimal structure for configuration 2 are shown in Fig. 14.

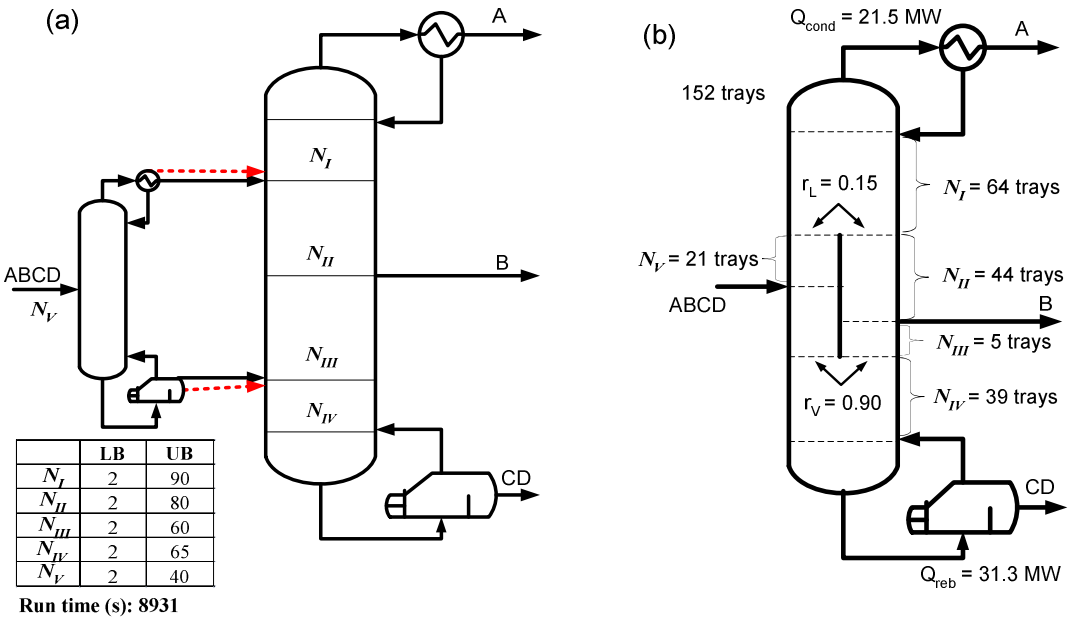

Figure 14: Model for DWC configuration 2 showing (a) simulation structure, with PSO variables and bounds (b) optimal structure of the equivalent DWC design with the condenser and reboiler duties, liquid split ratio (r_L) and vapor split ratio (r_V)

4.2.3 **DWC configuration 3**

In configuration 3, a 4-product DWC based on a Kaibel configuration is used. The additional product in this configuration means that in comparison to the 3-product DWC an extra operating variable needs to be specified for the operation of the column, and an extra discrete variable for optimizing the structure. The extra operating variable is the side stream flowrate of the additional side product, while an additional discrete variable is added to represent the column section between the two side products. Similar to the 3-product DWC configurations, the prefractionator operating variables are kept constant at their V_{min} values while the product column's operating variables are varied to meet product specifications during the process simulation. The number of trays in the prefractionator is given as the summation of variables N_{II} - N_{IV}, with the assumption that the number of trays in the prefractionator is equal to the number of trays in the

equivalent sections of the product column also being maintained. Fig. 15 shows the structure setup and optimal structure.

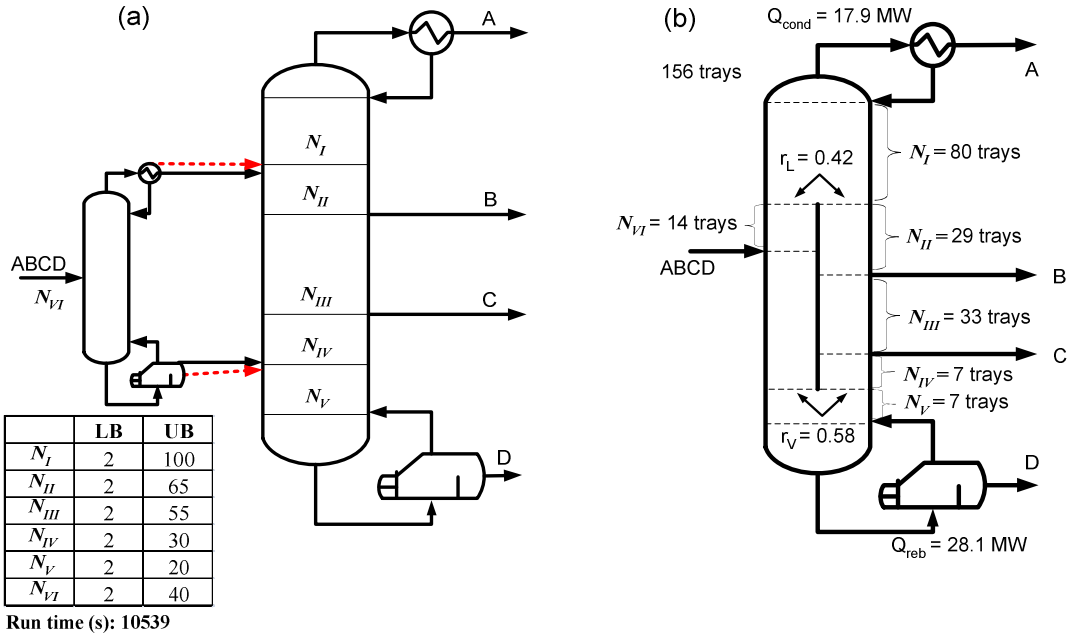

	LB	UB
N_I	2	100
N_{II}	2	65
N_{III}	2	55
N_{IV}	2	30
N_V	2	20
N_{VI}	2	40

Figure 15: DWC configuration 3 showing (a) simulation structure, with PSO variables and bounds (b) optimal structure of the equivalent DWC design with the condenser and reboiler duties, liquid split ratio (r_L) and vapor split ratio (r_V)

4.3 **Optimization results (economics)**

The economic results of all the cases studied are shown in Table 7. As can been seen, configurations 1 to 3 all have better economic results than the base case, with the least amount of savings experienced for configuration 1. This is because the methanol recovery column, which is the column with the most significant cost in the base case, also contributes to configuration 1. In configuration 3, the advantages of implementing all product recoveries in one DWC column is quite clear, as savings in TAC of up to 28 % in comparison to the base case are obtained. These savings are mainly as a result of huge savings (31 %) in operating costs obtained in this configuration. These results highlight the big potential that DWCs have in replacing conventional columns in the

separation section of the thermochemical biobutanol process. It is also conceivable that similar savings might be obtainable for other biofuel applications.

Table 7: Operating cost, capital cost and TAC results for all cases studied

Base case			
	Op. Cost (k$/yr)	Cap. Cost (k$)	TAC (k$/yr)
Methanol recovery column	2,075	1,550	2,484
Ethanol/propanol recovery column	513	681	693
Butanol recovery column	126	165	170
Total	2,714	2,396	3,346
Configuration 1			
	Op. Cost (k$/yr)	Cap. Cost (k$)	TAC (k$/yr)
Methanol recovery column	2,075	1,550	2,484
3-product DWC	579	755	778
Total	2,654	2,305	3,262
Savings with respect to base case	*2.2%*	*3.8%*	*2.5%*
Configuration 2			
	Op. Cost (k$/yr)	Cap. Cost (k$)	TAC (k$/yr)
3-product DWC	2,098	2,053	2,640
Butanol recovery column	126	165	170
Total	2,225	2,218	2,810
Savings with respect to base case	*18.0%*	*7.4%*	*16.0%*
Configuration 3			
	Op. Cost (k$/yr)	Cap. Cost (k$)	TAC (k$/yr)
4-product DWC	1,878	2,033	2,414
Savings with respect to base case	*30.8%*	*15.2%*	*27.9%*

4.4 **Sensitivity analysis on best configuration (configuration 3)**

As has been seen from the results obtained in the prior section, the best configuration for the separation is configuration 3, the 4-product DWC. In this section, a sensitivity

analysis on the results of configuration 3 is carried out on some of the key economic assumptions made in this work such as the depreciation time, interest rate, utility price and cost of the sieve trays in the dividing wall section, to see the effect of these parameters on the TAC and the column structure (number of trays). These results are shown graphically in Fig. 16, with the TAC trends shown with solid lines, and the number of trays trends shown with the hashed trend lines. The relationship between the TAC and number of trays versus the interest rate is shown in Fig. 16 (a). Increasing the interest rate increases the TAC, as the cost of borrowing capital becomes higher, while the opposite occurs when the interest rate is reduced. However, the number of trays in the column remains the same. In Fig. 16 (b), a plot of the change in TAC and number of trays with respect to annualization time is shown. As can be seen, an increase in annualization time from the base case results in a decrease in TAC and vice versa with a decrease in the annualization time. The increased annualization time means that capital cost repayments are spread over a longer time period, thus reducing the annualization factor and the contribution of the capital cost to the TAC, the opposite occurs when the annualization time is reduced. Note that the exponential relationship between the TAC and annualization time is a result of the exponential relationship between the annualization factor and annualization time as can be seen in equation (7).

The change in the number of trays follows a trend which is opposite to the change in TAC. This is because with an increase in annualization time, the cost of borrowing capital becomes cheaper thus favoring columns with more trays. In Fig. 16 (c), the TAC and optimal number of trays are plotted against the utility price. The values on the x-axis of this figure are percentage changes in utility (steam and cooling water) price from the base case values, with 100 % representing the base case. The plot shows that a linear direct relationship exists between the TAC and utility price as expected based on the

equations discussed in section 3.4. The change in the number of trays with respect to the utility price also follows a linear trend. This is because as the operating cost is increased, taller columns are favored and vice versa when the operating cost is reduced.

Finally, the TAC and number of trays are plotted against the cost factor assumed for the sieve trays in the dividing wall section of the DWC. As is seen in Fig. 16 (d), the relationship between the TAC and sieve tray factor is linear. Increasing the tray factor means that the sieve trays are more expensive for the DWCs thus causing an increase in the TAC, and vice versa when the tray factor is reduced. However, the change in the number of trays with respect to the tray factor is linear but opposite to the TAC. This is because smaller columns are favored when the cost of the sieve trays, and thus capital cost are increased. It should be noted that noise in the data is due to suboptimal results generated by the PSO, since the number of iterations was restricted to 100 for each case.

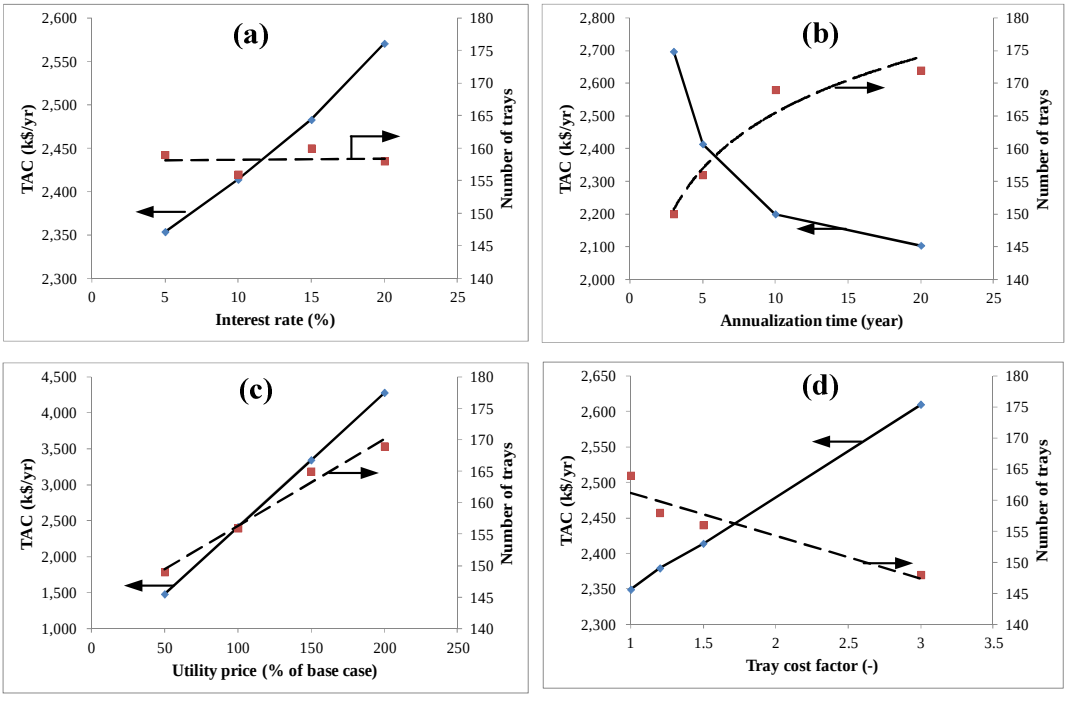

Figure 16: Sensitivity analysis on results of best configuration (configuration 3)

5. Conclusion

This work has looked at the design of DWC configurations for application to the separation section of a thermochemical biobutanol process. A general methodology based on the use of shortcut methods for column initialization, and a two-tier simulation - optimization strategy was discussed and used for design of the DWCs. The results show that all the DWC configurations provide cost savings in comparison to a base case configuration of three conventional columns in direct sequence. Furthermore, the 4-product DWC provides the most savings, with up to 31 % savings in operating costs, and 28 % savings in TAC. Note that these savings are reasonable and in line with the general savings reported for DWCs in other cases. Therefore, it can be concluded that the implementation of DWC technology in a thermochemical biobutanol process can lead to cost savings and thus improvements in the overall economics of the process. In future work the authors intend to carry out a full system study to quantify how the use of DWC configurations impact on the production cost of biobutanol from the thermochemical route.

6. Acknowledgement

This work was funded by an Ontario Research Fund – Research Excellence Grant (ORF RE-05-072)

Nomenclature

F feed flowrate (kmol/hr)

z composition

q feed quality, liquid fraction

V_T vapor flow in the top section of the column (kmol/hr)

D distillate (kmol/hr)

$N_{\min}$ minimum number of trays

L_T liquid flow at the top of the column (kmol/hr)

L_B liquid flow at the bottom of the column (kmol/hr)

V_B vapor flow at the bottom of the column (kmol/hr)

B bottoms flow rate (kmol/hr)

s tray spacing (m)

H column height (m)

NT number of trays

f annualization factor

i fractional interest rate per year

n annualization period in years (yr)

RR reflux ratios

BR boilup ratios

Dia column diameter (m)

N_j number of trays in the jth section of the product column

N_{feed} tray number of feed location

Q_{reb} reboiler duty (MW)

Q_{cond} condenser duty (MW)

T_{reb} reboiler temperature (℃)

T_{cond} condenser temperature (℃)

r_L liquid split ratio

r_V vapor split ratio

References

[1] International Energy Agency, World Energy Outlook 2013, 2013. http://www.worldenergyoutlook.org/media/weowebsite/2013/WEO2013_Ch06_Renewables.pdf.

[2] Ö. Yildirim, A. A. Kiss, E.Y. Kenig, Dividing wall columns in chemical process industry: A review on current activities, Sep. Purif. Technol. 80 (2011) 403–417.

[3] R. Agrawal, Z.T. Fidkowski, Are Thermally Coupled Distillation Columns Always Thermodynamically More Efficient for Ternary Distillations□?, 5885 (1998) 3444–3454.

[4] R.R. Rewagad, A. A. Kiss, Dynamic optimization of a dividing-wall column using model predictive control, Chem. Eng. Sci. 68 (2012) 132–142.

[5] N. Asprion, G. Kaibel, Dividing wall columns: Fundamentals and recent advances, Chem. Eng. Process. Process Intensif. 49 (2010) 139–146.

[6] A. A. Kiss, R.M. Ignat, Innovative single step bioethanol dehydration in an extractive dividing-wall column, Sep. Purif. Technol. 98 (2012) 290–297.

[7] A. A. Kiss, Distillation technology - still young and full of breakthrough opportunities, J. Chem. Technol. Biotechnol. 89 (2014) 479–498.

[8] L.Y. Sun, X.W. Chang, C.X. Qi, Q.S. Li, Implementation of Ethanol Dehydration Using Dividing-Wall Heterogeneous Azeotropic Distillation Column, Sep. Sci. Technol. 46 (2011) 1365–1375.

[9] I. Dejanović, L. Matijašević, Ž. Olujić, Dividing wall column—A breakthrough towards sustainable distilling, Chem. Eng. Process. Process Intensif. 49 (2010) 559–580.

[10] A. A. Kiss, C.S. Bildea, A control perspective on process intensification in dividing-wall columns, Chem. Eng. Process. Process Intensif. 50 (2011) 281–292.

[11] H. Ling, W.L. Luyben, New Control Structure for Divided-Wall Columns, Ind. Eng. Chem. Res. 48 (2009) 6034–6049.

[12] D. Dwivedi, J.P. Strandberg, I.J. Halvorsen, S. Skogestad, Steady state and dynamic operation of four-product dividing-wall (Kaibel) columns: Experimental verification, Ind. Eng. Chem. Res. 51 (2012) 15696–15706.

[13] M. Kumar, K. Gayen, Developments in biobutanol production: New insights, Appl. Energy. 88 (2011) 1999–2012.

[14] A. Ranjan, V.S. Moholkar, Biobutanol: science, engineering, and economics, Int. J. Energy Resour. 36 (2012) 277–323.

[15] C. Okoli, T.A. Adams II, Design and economic analysis of a thermochemical lignocellulosic biomass-to-butanol process, Ind. Eng. Chem. Res. 53 (2014) 11427–11441.

[16] A. A. Kiss, Novel applications of dividing-wall column technology to biofuel production processes, J. Chem. Technol. Biotechnol. 88 (2013) 1387–1404.

[17] A. A. Kiss, R.M. Ignat, Enhanced methanol recovery and glycerol separation in biodiesel production - DWC makes it happen, Appl. Energy. 99 (2012) 146–153.

[18] M. Ghadrdan, I.J. Halvorsen, S. Skogestad, Optimal operation of Kaibel distillation columns, Chem. Eng. Res. Des. 89 (2011) 1382–1391.

[19] I. Dejanović, L. Matijašević, I.J. Halvorsen, S. Skogestad, H. Jansen, B. Kaibel, et al., Designing four-product dividing wall columns for separation of a multicomponent aromatics mixture, Chem. Eng. Res. Des. 89 (2011) 1155–1167.

[20] I.J. Halvorsen, S. Skogestad, Minimum Energy Consumption in Multicomponent Distillation. 1. Vmin Diagram for a Two-Product Column, Ind. Eng. Chem. Res. 42 (2003) 596–604.

[21] I.J. Halvorsen, S. Skogestad, Minimum Energy Consumption in Multicomponent Distillation. 2. Three-Product Petlyuk Arrangements, Ind. Eng. Chem. Res. 42 (2003) 605–615.

[22] I.J. Halvorsen, S. Skogestad, Minimum Energy Consumption in Multicomponent Distillation. 3. More Than Three Products and Generalized Petlyuk Arrangements, Ind. Eng. Chem. Res. 42 (2003) 616–629.

[23] A. A. Kiss, R.M. Ignat, S.J. Flores Landaeta, A.B. De Haan, Intensified process for aromatics separation powered by Kaibel and dividing-wall columns, Chem. Eng. Process. Process Intensif. 67 (2013) 39–48.

[24] L. Sun, X. Bi, Shortcut method for the design of reactive dividing wall column, Ind. Eng. Chem. Res. 53 (2014) 2340–2347.

[25] J. Javaloyes-Antón, R. Ruiz-Femenia, J. A. Caballero, Rigorous Design of Complex Distillation Columns Using Process Simulators and the Particle Swarm Optimization Algorithm, Ind. Eng. Chem. Res. 52 (2013) 15621–15634.

[26] J. Leboreiro, J. Acevedo, Processes synthesis and design of distillation sequences using modular simulators: a genetic algorithm framework, Comput. Chem. Eng. 28 (2004) 1223–1236.

[27] M. Gendreau, J.-Y. Potvin, Handbook of Metaheuristics Vol. 2, Springer, New York, 2010.

[28] A. Kaveh, Advances in Metaheuristic Algorithms for Optimal Design of Structures, Springer, New York, 2014.

[29] A. Pascall, T. A. Adams II, Semicontinuous separation of dimethyl ether (DME) produced from biomass, Can. J. Chem. Eng. 91 (2013) 1001–1021.

[30] M.A. Navarro, J. Javaloyes, J.A. Caballero, I.E. Grossmann, Strategies for the robust simulation of thermally coupled distillation sequences, Comput. Chem. Eng. 36 (2012) 149–159.

[31] ASTM Standard D7862-15, Standard Specification for Butanol for Blending with Gasoline for Use as Automotive Spark-Ignition Engine Fuel, (2015). doi:10.1520/D7862-15.

[32] K. Ramakrishnan, P.L. Sabarethinam, Pet. Chem. Ind. Dev. 11 (1977) 19–22.

[33] J.M. Resa, C. Gonzalez, J.M. Goenaga, M. Iglesias, Density, Refractive Index, and Speed of Sound at 298.15 K and Vapor−Liquid Equilibria at 101.3 kPa for Binary Mixtures of Ethyl Acetate + 1-Pentanol and Ethanol + 2-Methyl-1-propanol, J. Chem. Eng. Data. 49 (2004) 804–808.

[34] A.S. Mozzhukhin, V.A. Mitropol'skaya, L.A. Serafimov, A.I. Torubarov, T.S. Rudakovskaya, Zhurnal Fiz. Khimii. 41 (1967) 227.

[35] K. Kojima, K. Tochigi, H. Seki, K. Watase, Determination of vapor-liquid equilibrium from boiling point curve, Kagaku Kogaku Ronbunshu. 32 (1968) 149–153.

[36] K. Kurihara, M. Nakamichi, K. Kojima, Isobaric vapor-liquid equilibria for methanol + ethanol + water and the three constituent binary systems, J. Chem. Eng. Data. 38 (1993) 446 – 449.

[37] K. Ochi, K. Kojima, Vapor-liquid equilibrium for ternary systems consisting of alcohols and water, Kagaku Kogaku Ronbunshu. 33 (1969) 352.

[38] W.D. Seider, J.D. Seader, D.R. Lewin, Product & Process Design Principles: Synthesis, Analysis and Evaluation, 3rd ed., John Wiley & Sons, Hoboken, New Jersey, 2009.

[39] A.K. Modi, A.W. Westerberg, Distillation column sequencing using marginal price, Ind. Eng. Chem. Res. 31 (1992) 839 – 848.

[40] G. Kaibel, Distillation columns with vertical partitions, Chem. Eng. Technol. 10 (1987) 92–98.

[41] Ž. Olujić, M. Jödecke, A. Shilkin, G. Schuch, B. Kaibel, Equipment improvement trends in distillation, Chem. Eng. Process. Process Intensif. 48 (2009) 1089–1104.

[42] T.A. Adams II, W.D. Seider, Practical optimization of complex chemical processes with tight constraints, Comput. Chem. Eng. 32 (2008) 2099–2112.

[43] S. Boubaker, M. Djemai, N. Manamanni, F. M'Sahli, Active modes and switching instants identification for linear switched systems based on Discrete Particle Swarm Optimization, Appl. Soft Comput. 14 (2014) 482–488.

[44] P.C. Wankat, Separations in chemical engineering: equilibrium staged separations., Elsevier, New York, 1988.

[45] U.E.I.A. EIA, Henry Hub Gulf Coast Natural Gas Spot Price, (2012). http://www.eia.gov/dnav/ng/hist/rngwhhdW.htm.

[46] I.E.S.O. IESO, Hourly Ontario Energy Price, (2012). http://www.ieso.ca/Pages/Power-Data/default.aspx.

[47] G. Towler, R. Sinnott, Chemical engineering design: principles, practice and economics of plant and process design, 2nd Edition, Butterworth-Heinemann, Massachusetts, 2012.

[48] G.P. Rangaiah, E.L. Ooi, R. Premkumar, A Simplified Procedure for Quick Design of Dividing-Wall Columns for Industrial Applications, Chem. Prod. Process Model. 4 (2009) 1–42.

[49] R. Smith, Chemical process design and integration, John Wiley & Sons, Chichester, 2005.

[50] I.J. Halvorsen, S. Skogestad, Minimum Energy for the four-product Kaibel-column, in: AIChE annual meeting, 2006.

[51] M. Ghadrdan, I.J. Halvorsen, S. Skogestad, A Shortcut Design for Kaibel Columns Based on Minimum Energy Diagrams, in: E.N. Pistikopoulos, M.C. Georgiadis, A.C. Kokossis (Eds.), 21st Eur. Symp. Comput. Aided Process Eng. ESCAPE 21, Elsevier B.V., Porto Carras, Greece, 2011: pp. 356 – 360.